Gaussian and Non-Gaussian Noise Effects on Data-Driven Modeling: A Comparative Investigation

Bemnet Wondimagegnehu Mersha[1][0000−0002−1000−8984], Yaping Dai[2][0000−0001−8795−5333], and Kaoru Hirota[3][0000−0001−5347−6182]

[1] School of Automation, Beijing Institute of Technology, Beijing, 100081, China email: MershaBemnetW@bit.edu.cn

[2] Beijing Institute of Technology Zhuhai, Tangjiawan, Zhuhai City, 519088, Guangdong, China email: daiyaping@bit.edu.cn

[3] School of Automation, Beijing Institute of Technology, Beijing, 100081, China email: hirota@bit.edu.cn

Abstract. To ensure reliable predictions for various applications, it is essential to understand the impact of Gaussian and non-Gaussian noise on data-driven modeling. Gaussian noise has been a convenient assumption for model development, but real-world scenarios sometimes defy Gaussian assumptions. Our research compared the performances of the direct and parametric data-driven modeling methods with Gaussian and non-Gaussian sensor noise. The direct data-driven modeling methods that are evaluated are direct data-driven methods with pulse input-output dataset and direct data-driven methods with step input-output dataset. The parametric models that are evaluated are the Output Error (OE), Autoregressive with Moving Average and Exogenous Input (ARMAX), Autoregressive with Exogenous Input (ARX) and Box-Jenkins model (BJ). The result shows that the performance of the direct and the parametric data-driven modeling methods deteriorates under non-Gaussian noise.

Keywords: Data-driven modeling · Gaussian Noise · non-Gaussian Noise · Model performance

1 Introduction

In order to simulate system dynamics and ensure that predictions are reliable and applicable to a wide range of applications, it is essential to comprehend how Gaussian and non-Gaussian noise affect data-driven modeling. For a considerable time, Gaussian noise with symmetrical and well-behaved properties has been a convenient assumption in model development. However, the real world frequently poses obstacles that defy Gaussian predictions, such as outliers, large tails, and asymmetrical distributions. The sensitivity of data-driven modeling techniques to non-Gaussian noise is crucial for making reliable and accurate predictions.

Models based purely on Gaussian assumptions may fail to capture the complexities of dynamical systems, resulting in inaccurate parameter estimations and inferior performance. In the realm of data-driven modeling, foundational approaches like the Output Error (OE), Autoregressive with Moving Average and Exogenous Input (ARMAX), Autoregressive with Exogenous Input (ARX), and Box-Jenkins model (BJ) have traditionally assumed Gaussian conditions. However, the growing recognition of the impact of non-Gaussian noise prompts a reevaluation of these methods.

Recent research introduces novel techniques that explicitly address non-Gaussian characteristics [1, 2] and has emphasized the importance of investigating the effects of non-Gaussian noise in data-driven modeling. Literature highlights how heavy-tailed noise affects parameter estimation accuracy [3], exposing possible flaws in traditional modeling techniques. The implications of non-Gaussian noise for volatility modeling are investigated in fields such as financial time series [4], illuminating the shortcomings of Gaussian-based noise assumptions in describing extreme occurrences. Robust techniques that can handle departures from Gaussian assumptions are essential, as evidenced by new insights into the difficulties presented by non-Gaussian noise in dynamic system data-driven modeling [2]. Some researchers also point out the necessity of evaluating the effect of non-Gaussian noise for parameter estimation methods in fault detection systems [5, 6].

Even though there are great advancements in machine learning and data science, most industrial applications use traditional data-driven modeling methods because of their simplicity and effectiveness compared to the complexity and implementation issues associated with machine learning models. For example, ARMAX is used for monitoring the internal level of large-scale renewable energy units in the grid [7]. Because dynamical systems are always time-varying, the model must adapt with time. The traditional data-driven methods like the Output Error (OE), Autoregressive with Moving Average and Exogenous Input (ARMAX), Autoregressive with Exogenous Input (ARX), and Box-Jenkins model (BJ) give simple but feasible results for many industrial applications [8, 9]. As a result, evaluating the traditional data-driven modelings under Gaussian and non-Gaussian noise has practical advantages for industrial processes.

The performance of conventional modeling techniques' response to Gaussian and non-Gaussian noise is evaluated. In-depth analysis of foundational approaches like the direct approach, Output Error (OE), Autoregressive with Moving Average and Exogenous Input (ARMAX), Autoregressive with Exogenous Input (ARX), and Box-Jenkins model (BJ) when the dataset for modeling has Gaussian and non-Gaussian noise is carried out. To aid the comparative analysis, we use the second-order system given by

$$H(z) = \frac{0.1129z + 0.1038}{z^2 - 1.562z + 0.7788}. \tag{1}$$

The whole comparative analysis is divided into two sections. First, we will evaluate the performance of direct pulse response estimation methods to Gaussian and non-Gaussian noise. Then, we present an in-depth evaluation of parametric data-driven methods under Gaussian and non-Gaussian noise.

2 Direct pulse response estimations techniques

The direct approach of data-driven modeling develops the dynamical system's impulse response using pulse response or step response data collected from the dynamical system. The input that can be used to collect the dataset can be either a scaled discrete pulse input (see Equation (2)) or a scaled step input (see equation (3)).

$$u[k] = \alpha\delta[k] = \begin{cases} \alpha, & k = 0 \\ 0, & k \neq 0 \end{cases}, \tag{2}$$

$$u[k] = \alpha s[k] = \begin{cases} \alpha, & k \geq 0 \\ 0, & k < 0 \end{cases}. \tag{3}$$

Here, k is the discrete time, $u[k]$ is the pulse input, α is a finite real number, $\delta[k]$ is the Dirac delta function and $s[k]$ is the unit step function.

If the data is collected using the scaled discrete pulse, the unit-pulse response coefficients can be estimated as:

$$\breve{g}[k] = \frac{y[k]}{\alpha} + \frac{v[k]}{\alpha}. \tag{4}$$

Here, $v[k]$ is a measurement noise and $\breve{g}[k]$ is the estimated unit-pulse response of the system. In order to reduce the effect of the noise, the value of α must be large enough to eliminate the noise. However, most systems do not allow large enough scaled pulse input to completely remove the effect of the noise.

If the scaled discrete step signal is used to collect the input-output data, the unit-pulse response can be given by

$$\breve{g}[k] = \frac{(y[k] - y[k-1])}{\alpha} + \frac{(v[k] - v[k-1])}{\alpha}. \tag{5}$$

The effect of the noise on the estimated unit-pulse response can be canceled if it is a slowly varying signal. If the noise is Gaussian, its effect will not be canceled. The direct data-driven modeling technique is not widely used. However, many engineers occasionally employ it to gain an overview of any black box system.

To evaluate the performance of the direct approach to Gaussian and non-Gaussian noise, input-output data is collected using pulse and step input from the discrete dynamic system given in Equation 1. In practice, the transfer function of the system is unknown, and the data will be collected from the dynamic system. Then, the unit-pulse response is estimated using the direct approach. In the first experiment, a Gaussian noise of zero mean and variance of 0.01

($\mathcal{N}(0, 0.01)$) is added to the input-output data. In the second experiment, a Gaussian noise of zero mean and variance of 0.05 ($\mathcal{N}(0, 0.05)$) was added to the input-output dataset. In the third experiment, a correlated noise (non-Gaussian noise) is added to the input-output dataset. The non-Gaussian noise is generated by filtering Gaussian noise through a low-pass filter. The low-pass filter has a pole at $0.9312 \pm 0.3436i$.

3 Parametric data-driven techniques

As the size of the unit-pulse response increases, the difficulty of estimating the unit-pulse response increases. Parametric data-driven modeling attempts to reduce the number of parameters that must be estimated. The parametric data-driven modeling technique begins with the assumption of a transfer function of the dynamic system to decrease the number of parameters estimated. The general transfer function model for the parametric data-driven techniques is given by:

$$
\begin{aligned}
y[k] &= G(q)u[k] + H(q)e[k], i.e., \\
G(q) &= \frac{B(q)}{A(q)} \; and \; H(q) = \frac{C(q)}{D(q)}
\end{aligned}
\tag{6}
$$

where $G(q)$ is the transfer function for the input and $H(q)$ is the transfer function for the noise in the system. In parametric data-driven modeling $A(q)$, $B(q)$, $C(q)$ and $D(q)$ will be identified provided that they exists and n_k (the number of delays), n_a (the order of $A(q)$), n_b (the order of $B(q)$), n_c (the order of $C(q)$) and n_d (the order of $D(q)$) will also be determined. q is a time-domain one-period advance operator (q^{-1} is a time-domain one-period delay operator). The standard parametric data-driven modeling forms are the OE model, the ARMAX, the ARX, and the BJ.

The OE standard form is given by:

$$
\begin{aligned}
G(q,\theta) &= \frac{B(q,\theta)}{A(q,\theta)}, H(q,\theta) = 1, \\
y[k] &= \frac{B(q,\theta)}{A(q,\theta)} u[k] + e[k], \\
\theta &= \left[a_1 \ldots a_{n_a} b_1 \ldots b_{n_b}\right], \\
A(q,\theta) &= 1 + a_1 q^{-1} + \ldots + a_{n_a} q^{-n_a}, \\
B(q,\theta) &= 1 + b_1 q^{-1} + \ldots + b_{n_b} q^{-n_b}
\end{aligned}
\tag{7}
$$

The ARMAX standard form is given by:

$$
\begin{aligned}
&G(q,\theta) = \frac{B(q,\theta)}{A(q,\theta)}, H(q,\theta) = \frac{C(q,\theta)}{A(q,\theta)},\\
&A(q,\theta)y[k] = B(q,\theta)u[k] + C(q,\theta)e[k],\\
&\theta = [a_1 \dots a_{n_a} b_1 \dots b_{n_b}],\\
&A(q,\theta) = 1 + a_1 q^{-1} + \dots + a_{n_a} q^{-n_a},\\
&B(q,\theta) = 1 + b_1 q^{-1} + \dots + b_{n_b} q^{-n_b},\\
&C(q,\theta) = 1 + c_1 q^{-1} + \dots + c_{n_c} q^{-n_c}.
\end{aligned}
\tag{8}
$$

The ARX standard form is given by:

$$
\begin{aligned}
&G(q,\theta) = \frac{B(q,\theta)}{A(q,\theta)}, H(q,\theta) = \frac{1}{A(q,\theta)},\\
&A(q,\theta)y[k] = B(q,\theta)u[k] + e[k],\\
&\theta = [a_1 \dots a_{n_a} b_1 \dots b_{n_b}],\\
&A(q,\theta) = 1 + a_1 q^{-1} + \dots + a_{n_a} q^{-n_a},\\
&B(q,\theta) = 1 + b_1 q^{-1} + \dots + b_{n_b} q^{-n_b}.
\end{aligned}
\tag{9}
$$

The BJ standard form is given by:

$$
\begin{aligned}
&G(q,\theta) = \frac{B(q,\theta)}{A(q,\theta)}, H(q,\theta) = \frac{C(q,\theta)}{D(q,\theta)},\\
&y[k] = \frac{B(q,\theta)}{A(q,\theta)}u[k] + \frac{C(q,\theta)}{D(q,\theta)}e[k].\\
&\theta = [a_1 \dots a_{n_a} b_1 \dots b_{n_b} c_1 \dots c_{n_c} d_1 \dots d_{n_d}],\\
&A(q,\theta) = 1 + a_1 q^{-1} + \dots + a_{n_a} q^{-n_a},\\
&B(q,\theta) = 1 + b_1 q^{-1} + \dots + b_{n_b} q^{-n_b},\\
&C(q,\theta) = 1 + c_1 q^{-1} + \dots + c_{n_c} q^{-n_c},\\
&D(q,\theta) = 1 + d_1 q^{-1} + \dots + d_{n_d} q^{-n_d}.
\end{aligned}
\tag{10}
$$

3.1 Parameter estimation and tests for the parametric data-driven techniques

Initializing the order of the model is the first stage in creating a data-driven parametric model of a system. The quickest method for estimating the delay (n_k) is to use the cross-correlation between the output and the input and count the number of periods it takes the signal to rise above the noise floor. To estimate the system model order (n_a, n_b, n_c *and* n_d), the simplest thing to do is to use frequency input-output data and estimate the order of the system from the bode plot.

To determine the model's parameters for prediction purposes, the least-square solution is used. The modeling error (residual) for a 1-step a head prediction is given by

$$\epsilon[k] = y[k] - \hat{y}[k|k-1] \tag{11}$$

where $\hat{y}[k|k-1]$ is the predicted value of the output at time k given measurements of the output up until (and including) time $k-1$. The least-square cost function ($V(\theta)$) can be given by:

$$\begin{aligned} V_N(\theta) &= \sum_{k=1}^{N} \epsilon^2[k;\theta], \\ \hat{\theta} &= arg\min_{\theta} V_N(\theta). \end{aligned} \tag{12}$$

The least-square solution for the ARX, ARMAX, OE, and BJ is described in [10, 11].

Several tests can be performed to validate models. The first desirable quality of the residue is that it is normally distributed and has a zero mean (at least symmetric). Typically, the residue's histogram is used to examine this. We can also try to estimate the residuals' variance (σ^2)

$$\sigma^2 = \frac{1}{N}\sum_{k=1}^{N} \epsilon^2[k] \tag{13}$$

The residue whiteness test (autocorrelation of the residue signal) is calculated using the following Equation:

$$\hat{R}_{\epsilon}^{N}[\tau] = \frac{1}{N}\sum_{k=1}^{N} \epsilon[k]\epsilon[k-\tau]. \tag{14}$$

We desire the autocorrelation of the residue to be zero at all values of $\tau \neq 0$. If it is zero, the model has successfully acquired all of the required data in the input-output dataset. This is demonstrated by assessing:

$$r_{N,M} = \frac{\sqrt{N}}{\hat{R}_{\epsilon}[0]}\left[\hat{R}_{\epsilon}[1]\ \hat{R}_{\epsilon}[2]\ \ldots\ \hat{R}_{\epsilon}[M]\right]^T \tag{15}$$

Then, according to the central limit theorem, as $N \to \infty$, $r_{N,M}$ will be normally distributed with zero mean and unit variance [10, 11]. If we sum together squares of $r_{N,M}$, the resulting function is

$$\zeta_{N,M} = \frac{N}{\left(\hat{R}_{\epsilon}^{N}[0]\right)^2}\sum_{\tau=1}^{M}\left(\hat{R}_{\epsilon}^{N}[\tau]\right)^2. \tag{16}$$

This is a chi-squared distribution with n degrees of freedom [10]. The overall test resides in checking if the chi-squared distribution is $\chi^2(M)$. That is, by checking

$\zeta_{N,M} < \chi^2_\alpha(M)$. For 95% confidence interval, we can use the ± 1.96 bounds on each element of $r_{N,M}$ [10].

The cross-correlation test assesses the correlation between the input and residual data by employing Equation (17). If the input is correlated with the residual values, the estimated model did not capture the relationship in the input-output data.

$$\hat{R}^N_{\epsilon u}[\tau] = \frac{1}{N}\sum_{k=1}^{N} \epsilon[k]u[k-\tau]. \tag{17}$$

We desire $\hat{R}^N_{\epsilon u}[\tau]$ to be roughly zero for $\tau > 0$. As $N \to 0$ it can be shown that $\sqrt(N)\hat{R}_{\epsilon u}[\tau]$ is normally distributed, with zero mean and variance $P_r = \sum_{-\infty}^{\infty} R_\epsilon[k]R_u[k]$. Normality test on $\hat{R}_{\epsilon u}[\tau]$ can be performed by checking $|\hat{R}_{\epsilon u}[\tau]| \leq 1.96\sqrt{(\frac{P_r}{N})}$ for all τ [10].

4 Result and Analysis of the Experiment

4.1 The performance of direct pulse response estimations techniques to Gaussian and non-Gaussian noise.

The performance of the direct pulse response estimation techniques deteriorates under non-Gaussian noise. Figure 1 shows that noise has a big impact on the direct data-driven modeling technique. As can be seen from Figure 1, the direct data-driven modeling can't give good modeling in the presence of very small Gaussian noise and non-Gaussian noise. As the Gaussian noise variance is increased from 0.01 to 0.05, the performance of the direct pulse response estimation techniques deteriorates. In the case of non-Gaussian noise, the performance of the direct pulse response estimation technique deteriorates further. This shows that the direct pulse response estimation techniques face challenges under non-Gaussian noise.

4.2 The performance of parametric data-driven techniques under Gaussian and non-Gaussian noise

The parametric data-driven modeling method is used to identify the system given in Equation (1) with Gaussian and non-Gaussian sensor noise. The non-Gaussian sensor noise was generated by passing a Gaussian noise through a low-pass filter. The low-pass filter has a pole at $0.9312 \pm 0.3436i$. The signal-to-noise power is set to 0.25%. Several tests are performed on the error (residual) to quantify the validity of the data-driven models. The mean and variance test on the residue, the whiteness test on the residue and the cross-correlation test between the residue and the input are the most prevalent tests. The performance of the parametric data-driven modeling result with the Gaussian and non-Gaussian sensor noise is shown in Table 1, Table 2, Figure 3, Figure 5, Figure 2, Table 3, Table 4 and

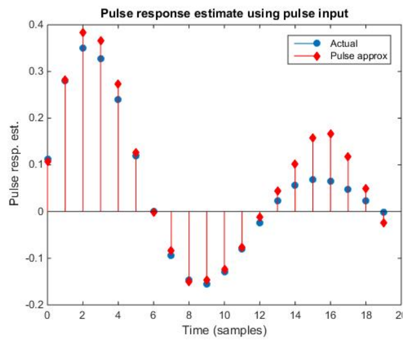

(a) Pulse input-output dataset with Gaussian ($\mathscr{N}(0, 0.01)$)

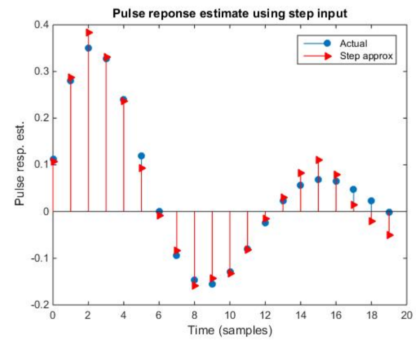

(b) Step input-output dataset with Gaussian ($\mathscr{N}(0, 0.01)$)

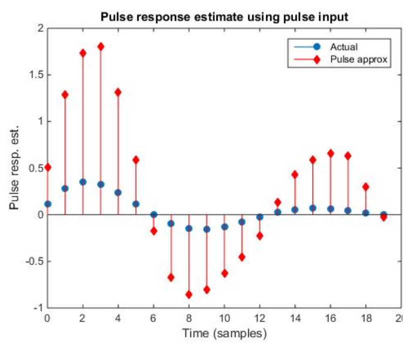

(c) Pulse input-output dataset with Gaussian ($\mathscr{N}(0, 0.05)$)

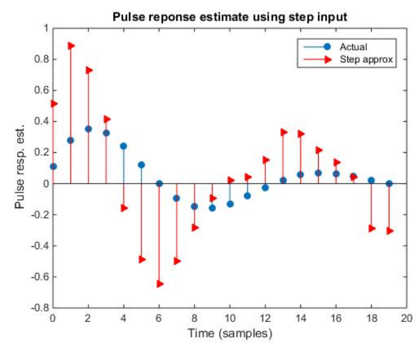

(d) Step input-output dataset with Gaussian ($\mathscr{N}(0, 0.05)$)

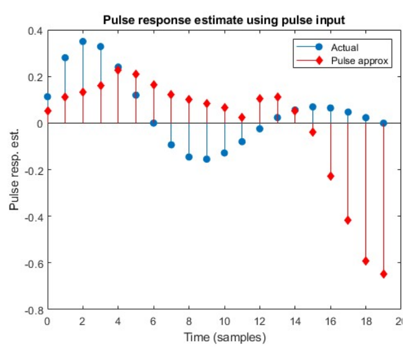

(e) Pulse input-output dataset with non-Gaussian

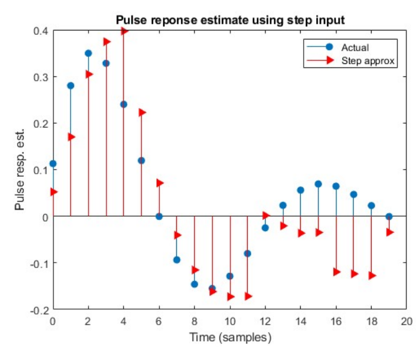

(f) Step input-output dataset with non-Gaussian

Fig. 1: Direct data-driven modeling with Gaussian noise and non-Gaussian noise

Table 5. The autocorrelation and cross-correlation plots in Figure 3 show that the autocorrelation of OE has 20 values and ARX has 5 values beyond the 95% confidence intervals. This shows that the residual value of the ARX model has correlations with the input and with itself, showing that the model did not fully capture the input-output data. ARMAX model performs better than OE and ARX. The performance of BJ is comparatively better than that of the other models.

In the case of the non-gaussian sensor noise case, it can be observed that the bode phase plots in Figure 5 above the cross-over frequency did not capture the actual model response. The one that has closer performance in the bode phase plot above the cross-over frequency is again the BJ model. In Table 1, Table 3, and Table 4, we also see that the BJ has close parameter values to the actual model compared with the other parametric models because the BJ model uses unique poles and zeros for modeling the effect of the reference input and the noise input. In the case of non-gaussian noise, the performance of all the model's frequency response plots shows it can not capture the high-frequency response of the actual plant.

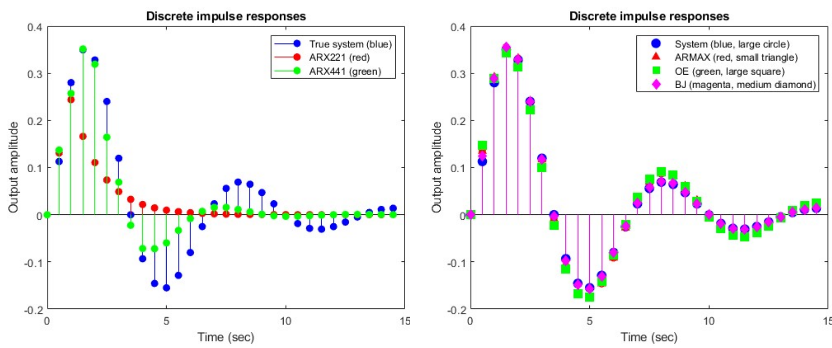

(a) ARX (b) BJ, ARMAX and OE

Fig. 2: Discrete Impulse Responses

Table 1: Parameter of $G(q)$ for Gaussian Noise case

	b_0	b_1	b_2	a_0	a_1	a_2
Actual	0	0.1129	0.1038	1	-1.562	0.7788
ARX	0	0.1309	0.1538	1	-0.689	0.0154
ARMAX	0	0.1144	0.0941	1	-1.569	0.787
BJ	0	0.1153	0.0940	1	-1.569	0.7872
OE	0	0.1148	0.0948	1	-1.568	0.7869

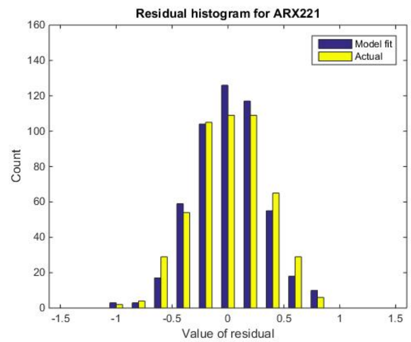

(a) Rresidual Histogram for ARX

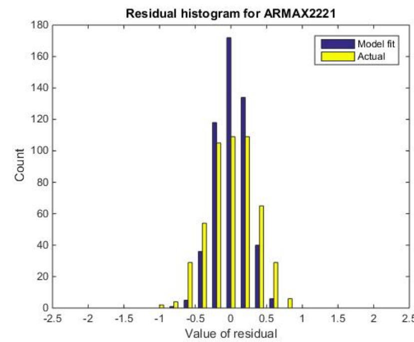

(b) Rresidual Histogram for ARMAX

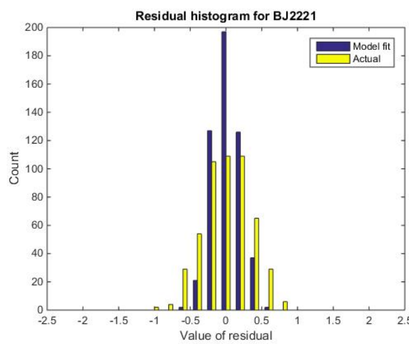

(c) Rresidual Histogram for BJ

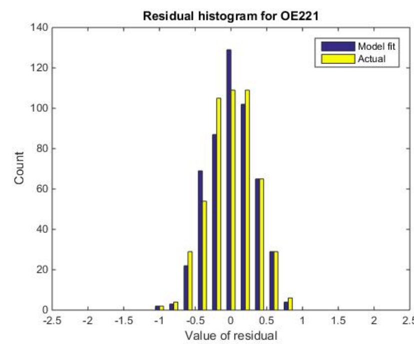

(d) Rresidual Histogram for OE

Fig. 3: Rresidual Histogram

Table 2: Mean and Variance for Gaussian Noise Case

	Atual	ARX	ARMAX	BJ	OE
Mean	-0.0221	-0.0087	-0.0272	-0.0281	-0.0249
Variance	0.1118	0.2206	0.1085	0.1091	0.1083

Table 3: Parameter of $G(q)$ for Non-Gaussian Noise case

	b_0	b_1	b_2	a_0	a_1	a_2
Actual	0	0.1129	0.1038	1	-1.562	0.7788
ARX221	0	0.1200	0.1106	1	-1.199	0.4338
ARMAX2221	0	0.1181	0.0868	1	-1.581	0.7984
BJ22221	0	0.1125	0.1002	1	-1.566	0.7841
OE221	0	0.1053	0.0920	1	-1.573	0.7889

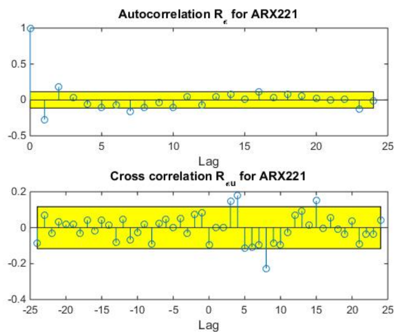

(a) Correlation plots of ARX

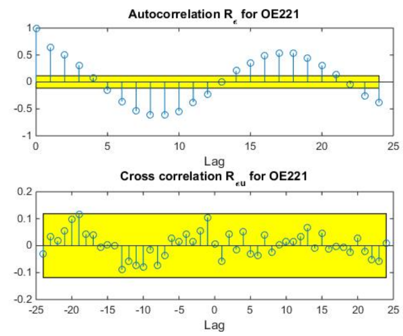

(b) Correlation plots of OE

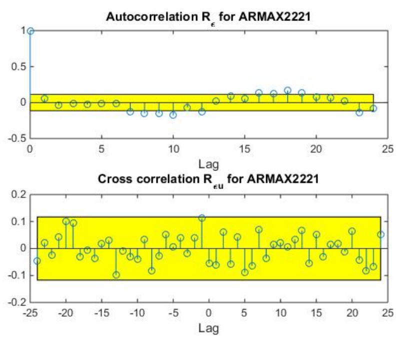

(c) Correlation plots of ARMAX

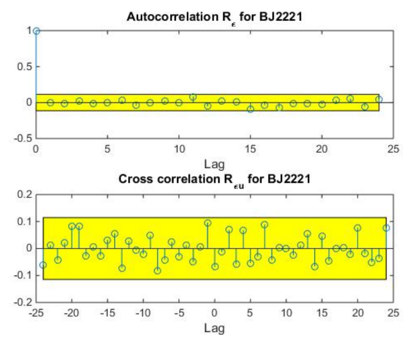

(d) Correlation plots of BJ

Fig. 4: Autocorrelation and Cross correlation

Table 4: Parameter of $H(q)$ for Non-Gaussian Noise case

	c_0	c_1	c_2	d_0	d_1	d_2
Actual	1	-1.634	0.7567	1	-1.862	0.9851
ARX221	1	0	0	1	-1.199	0.4338
ARMAX2221	1	-1.122	0.5905	1	-1.581	0.7984
BJ22221	1	-1.673	0.7865	1	-1.872	0.9955
OE221	1	0	0	1	0	0

Table 5: Mean and Variance for Non-Gaussian Noise Case

	Atual	ARX	ARMAX	BJ	OE
Mean	-0.0117	-0.0026	-0.0071	-0.0155	-0.0197
Variance	0.0310	0.0750	0.1085	0.0302	0.1038

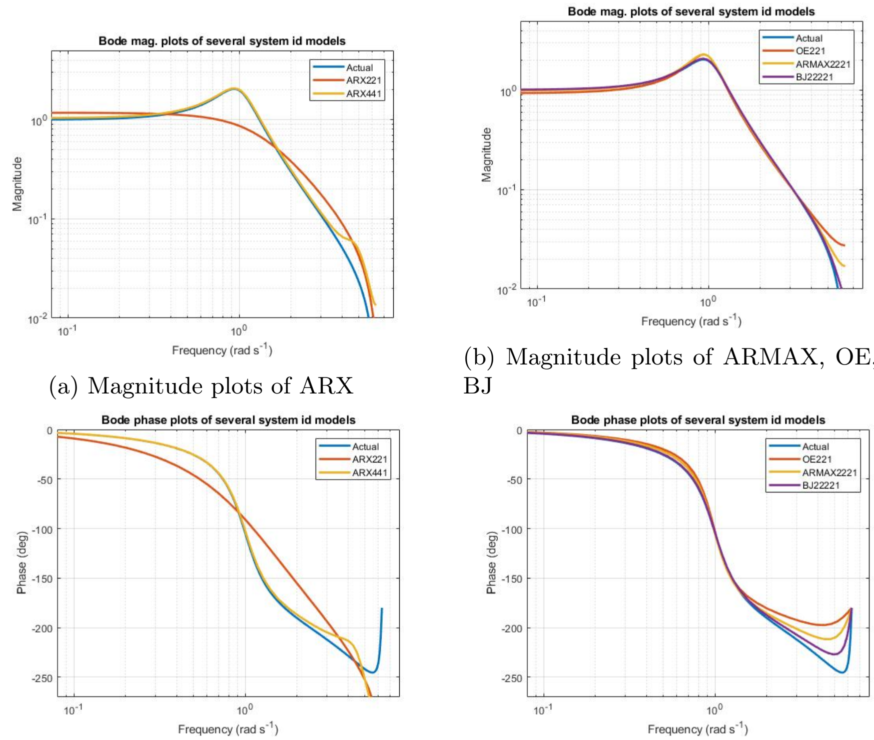

(a) Magnitude plots of ARX

(b) Magnitude plots of ARMAX, OE, BJ

(c) Phase plots of ARX

(d) Phase plots of ARMAX, OE, BJ

Fig. 5: Bode plot of the parametric data-driven models with Non-Gaussian sensor noise

5 Conclusion

In this research, we evaluated the performance of commonly used data-driven methods like the direct approach and the parametric approach to Gaussian and non-Gaussian noise. As the variance of the Gaussian noise increases from 0.01 to 0.05, the performance of the direct pulse response estimation techniques deteriorates. When the noise power is slightly increased by 5%, the method is not able to determine the actual system. The direct approach with step input-output data performed better than the direct approach with pulse input-output dataset to both Gaussian and non-Gaussian noise. In the case of the parametric data-driven modeling methods, the BJ data-driven modeling gave a better result. However, in the case of non-Gaussian noise, the performance is not good enough, especially above the cross-over frequency (Higher frequency). The performance of OE also deteriorates under non-Gaussian noise because it assumes that the noise enters the system without being filtered. Additionally, these methods assume a specific form for the dynamical system, which may not always fit the underlying characteristics of the system and the Gaussian/non-Gaussian noise that affects the actual system.

Bibliography

[1] Q. Zhang and Y. Zhou, "Recent advances in non-Gaussian stochastic systems control theory and its applications," *International Journal of Network Dynamics and Intelligence*, pp. 111–119, 2022.

[2] Y. Li and J. Duan, "A data-driven approach for discovering stochastic dynamical systems with non-Gaussian Lévy noise," *Physica D: Nonlinear Phenomena*, vol. 417, p. 132830, 2021.

[3] J. Chen, M. K. Ng, and D. Wang, "Quantizing heavy-tailed data in statistical estimation:(near) minimax rates, covariate quantization, and uniform recovery," *IEEE Transactions on Information Theory*, 2023.

[4] Y. Girgin, "Modeling exchange rate volatility using ARMA-GARCH aproach with non-Gaussian distributions," Master's thesis, Middle East Technical University, 2023.

[5] V. Stojanovic and D. Prsic, "Robust identification for fault detection in the presence of non-Gaussian noises: application to hydraulic servo drives," *Nonlinear Dynamics*, vol. 100, pp. 2299–2313, 2020.

[6] V. Stojanovic, S. He, and B. Zhang, "State and parameter joint estimation of linear stochastic systems in presence of faults and non-Gaussian noises," *International Journal of Robust and Nonlinear Control*, vol. 30, no. 16, pp. 6683–6700, 2020.

[7] Y. Liu, M. Sun, J. Wang, B. Liao, and J. Wu, "Inertia estimation of nodes and system based on armax model," in *2024 IEEE 2nd International Conference on Power Science and Technology (ICPST)*, pp. 401–407, 2024.

[8] P. Resma Madhu and J. Subbaiah, "Investigation of various data-driven modeling techniques for an industrial heat exchanger," in *International Conference on Data Management, Analytics & Innovation*, pp. 563–580, Springer, 2024.

[9] T. Tripura and S. Chakraborty, "A sparse bayesian framework for discovering interpretable nonlinear stochastic dynamical systems with gaussian white noise," *Mechanical Systems and Signal Processing*, vol. 187, p. 109939, 2023.

[10] L. Lennart, "System identification: theory for the user," *PTR Prentice Hall, Upper Saddle River, NJ*, vol. 28, p. 540, 1999.

[11] L. Scales, *Introduction to non-linear optimization.* Macmillan International Higher Education, 1985.